The Subcellular Origin of Bioluminescence in *Noctiluca miliaris*

ROGER ECKERT and GEORGE T. REYNOLDS

From the Department of Zoology, Syracuse University, New York, the Marine Biological Laboratory, Woods Hole, Massachusetts, and the Palmer Physical Laboratory, Princeton University, New Jersey

ABSTRACT The light emitted by *Noctiluca* has its origin in 1 to 5 × 10^4 organelles ("microsources") which are scattered throughout the perivacuolar cytoplasm, and which appear to be the elementary functional units of bioluminescence. Microscopical techniques, image intensification, and microphotometry were employed in their investigation. Microsources are fluorescent, strongly phase-retarding, and range widely in diameter below 1.5 microns. The number of quanta emitted in a flash from a microsource ("microflash") is of the order of 10^5 photons. However, microflashes show a wide range of intensities, which are correlated with the size of the organelles from which they arise. Each organelle responds repetitively and with reproducible time course to a succession of invading triggering potentials. Reversible changes in the intensity of the flash emitted by the whole cell ("macroflash") occur because of graduations in intensity of microflashes rather than as a result of changes in the number of responsive organelles. The shape of the flash emitted by individual microsources resembles that of the macroflash except for slightly shorter rise and decay times. It is concluded that the macroflash results from somewhat asynchronous, but otherwise parallel summation of microflashes.

INTRODUCTION

The response of luminescent dinoflagellates to mechanical stimulation is a transient emission with an intensity-time curve reminiscent of the tension-time curve of a muscle twitch (Nicol, 1958; Hastings, 1959; Eckert, 1965 *a*). Recent studies have shown that the flash of *Noctiluca miliaris* is triggered by an all-or-none action potential which propagates nondecrementally from the stimulated region of the cell over the remainder of the perivacuolar cytoplasm. As the action potential is conducted over a given region it is followed, after a latency of 2 to 3 msec, by the initial signs of light emission. Luminescence is thereby initiated over the cell in a progressive manner, beginning at the site of stimulation (Eckert, 1965 *a*, *b*).

When observed at low magnification, luminescence appears to arise dif-

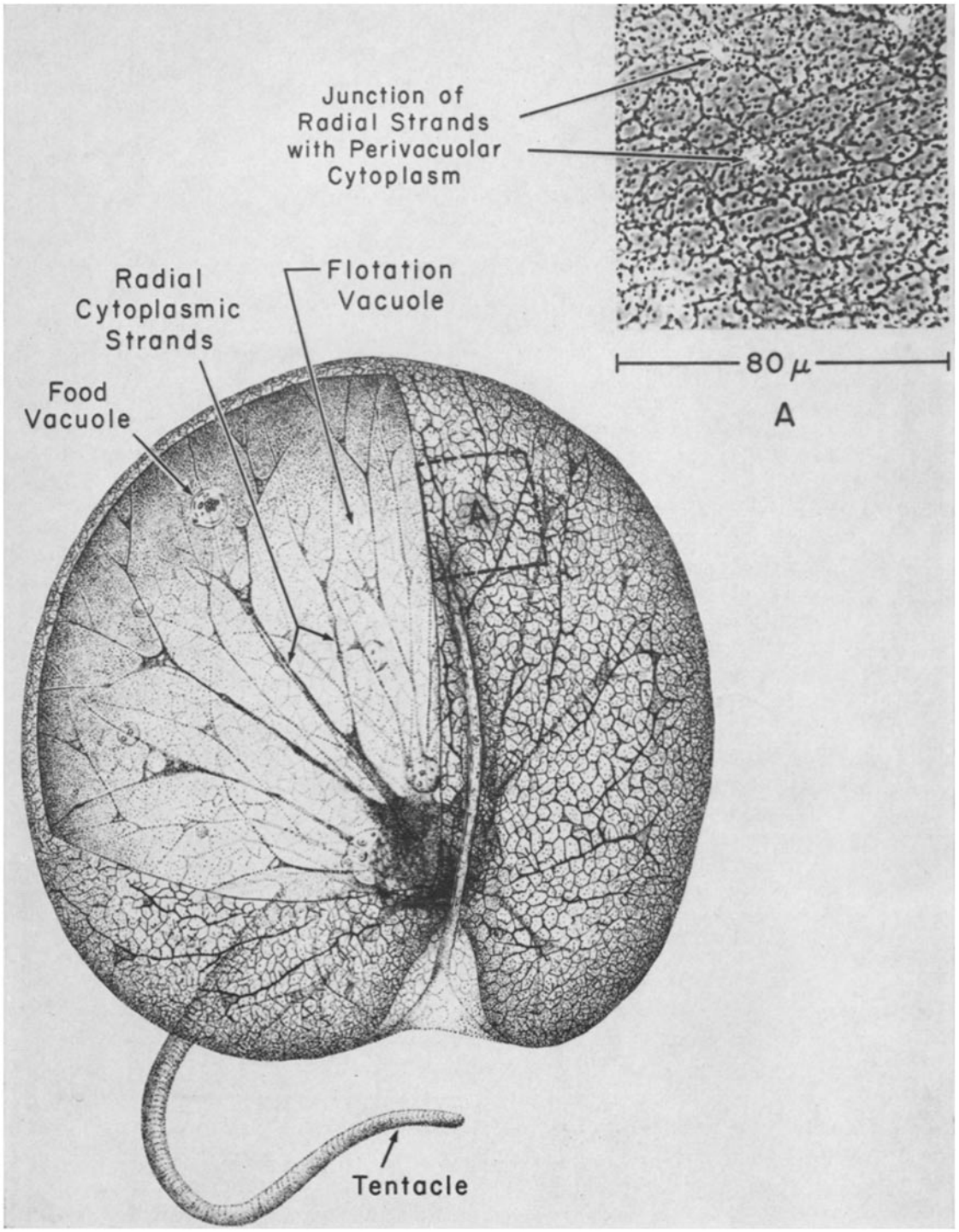

FIGURE 1. *Noctiluca miliaris*. Specimen is drawn with a hemiquadrant removed to expose internal features. The flotation vacuole occupies the bulk of cellular volume, and

fusely from the cell periphery. However, microscopical observation at high magnification reveals that the luminescence originates in numerous discrete and minute sources (Quatrefages, 1850; Harvey, 1917). The *macroflash* recorded from the entire cell is therefore the sum of many *microflashes*, each one of which originates in a separate organelle. We have investigated the behavior of the microsources of luminescence by several techniques, including microphotometry and autophotography by image intensification.

The light-emitting organelles vary in diameter below 1.5 μ and are located almost exclusively in the peripheral cytoplasm. The evidence indicates that in its sweep over the cell, the action potential (or an intimately associated event) elicits an independent emission from each individual microsource. This organelle, therefore, appears to be the functional and morphological unit of luminescence in *Noctiluca*, and most probably represents the level at which the mechanism of excitation-flash coupling functions (Eckert, 1965 *b*; 1966 *a,b*; Eckert et al., 1965).

The experiments and observations presented here demonstrate: (*a*) the identity of microsources with respect to cytoplasmic structures visible in the light microscope; (*b*) the fluorescence of the organelles; (*c*) the numbers and size distribution of microsources; (*d*) the quantum content of microflashes; (*e*) the one-to-one response of microsources to invading action potentials; (*f*) similarities in wave shape, time course, and intensity graduations between the microflash and macroflash, which indicate that the macroflash results primarily from spatial summation of microflashes.

METHODS AND MATERIALS

Cultures of *Noctiluca miliaris* have been maintained for several years under an illumination of 50 ft-c at 17° to 19°C in Pyrex dishes containing approximately 50 ml of autoclaved natural sea water. They were fed at intervals from an axenic culture of the marine alga *Dunaliella*. Reproduction occurred by simple binary fission at intervals of several days. The organism is an unarmored dinoflagellate, subreniform to spheroid in shape, ranging in diameter in our cultures from 300 to 600 μ (Fig. 1). The major morphological deviation from the typical dinoflagellate plan is the presence of the tentacle and the absence of a girdle, which is apparently due to inflation of the cell by

is traversed by numerous radial strands of cytoplasm which connect with the perivacuolar cytoplasm beneath the pellicle (not visible here). Both the radial strands and the perivacuolar cytoplasm show considerable structural lability. The organism ranges from 300 to more than 600 μ in diameter and ranges in shape from spherical to subreniform. The tentacle serves both to capture microorganisms in a mucoid secretion, and to convey them by bending movements to the cytostome.

Inset A. Phase-contrast photomicrograph of surface showing strandlike thickenings of perivacuolar layer of cytoplasm, light grey areas of sparse cytoplasm, and dark-looking, strongly phase-retarding round bodies (SPRB's). Straight, thin structures about 10 μ in length are discharged trichocysts (Sweeney and Bouck, 1966). The pellicle is not readily visualized with light microscopy.

a flotation vacuole which occupies the major portion of the cellular volume. The cytoplasm is distributed between a thin perivacuolar layer squeezed between the pellicle and the membrane which limits the floatation vacuole, a "central" perinuclear mass near the cytostome, and numerous fine labile radial strands within the vacuole connecting the central and perivacuolar cytoplasms. The morphology of *Noctiluca* is described in greater detail by Kofoid and Swezy (1921), Pratje (1921), and Gross (1934).

Three major methods were used to investigate the microsources and their luminescence in live specimens of *Noctiluca*: fluorescence and phase-contrast microscopy, autophotography by means of image intensification, and high-resolution photometry. Observations and experiments were performed on individual specimens in sea water at temperatures of 20° to 25°C. Specimens were immobilized for observation by a holding pipette with a terminal inside diameter of about 70 μ. Hydrostatic pressure, created by a 3–5 mm water level differential, served to hold the specimen to the opening of the pipette. Stimulating current to excite the immobilized cell was delivered through the same pipette. The bioelectric response has been described elsewhere (Eckert, 1965 *a*, *b*).

Microscopy was carried out with a Zeiss photomicroscope. A Zeiss 100 × planapochromat oil immersion phase-contrast objective of numerical aperture 1.30 was used for phase-contrast and fluorescence photography, and a Zeiss 100 × Neofluar oil immersion phase-contrast objective of NA 1.30 for microphotometric measurements. A Zeiss inverted microscope equipped with the 100 × Neofluar objective or a 40 × apochromat oil immersion phase objective of NA 1.0 was employed for the autophotography experiments. Light for fluorescence micrography was obtained from a 200 watt high pressure mercury lamp and was passed through a filter combination transmitting primarily the 365 and 404 mμ peaks. The barrier filter had a short wavelength cutoff at about 525 mμ. Simultaneous phase-contrast and fluorescence illuminations of variable ratio were obtained by the use of a Zeiss achromatic-aplanatic phase-contrast fluorescence condenser equipped with annular stops made of polarizing foil. The unpolarized ultraviolet illumination was largely unattenuated by the annular stop, whereas the tungsten light had been polarized at 90° with respect to the annular stop.

Autophotography of microsources by their emission was made possible by the use of an image intensifier tube, manufactured by the English Electric Company (Chelmsford, England). The major features of the IIT are shown diagrammatically in Fig. 2, and technical details are given elsewhere (Reynolds, 1964). The tube was operated at 36 kv for an intensification factor of 8.0 ($\pm$1.0) × 10^5; that is to say, an average of the order of 8 × 10^5 photons was emitted from the output phosphor for each photon impinging on the photocathode.

As a result of the limited number of photons from the specimen reaching the photocathode of the image tube and giving rise to photoelectrons (approximately 1 %), the intensified image showed considerable graininess. Additional "noise" in the image arose from thermal liberation of electrons in the first stage, and reflection of photons between the cathode and first dynode. Other sources of image noise were light scattering and reflection at interfaces of the optical system and experimental chamber, and

scattering within the specimen. Finally, there was a diffuse background of luminescence recorded with each flash, presumably having its origin in microsources at the far side of the cell, several hundred microns below the plane of microscope focus. The aggregate noise resulting from all these causes will collectively be termed "image

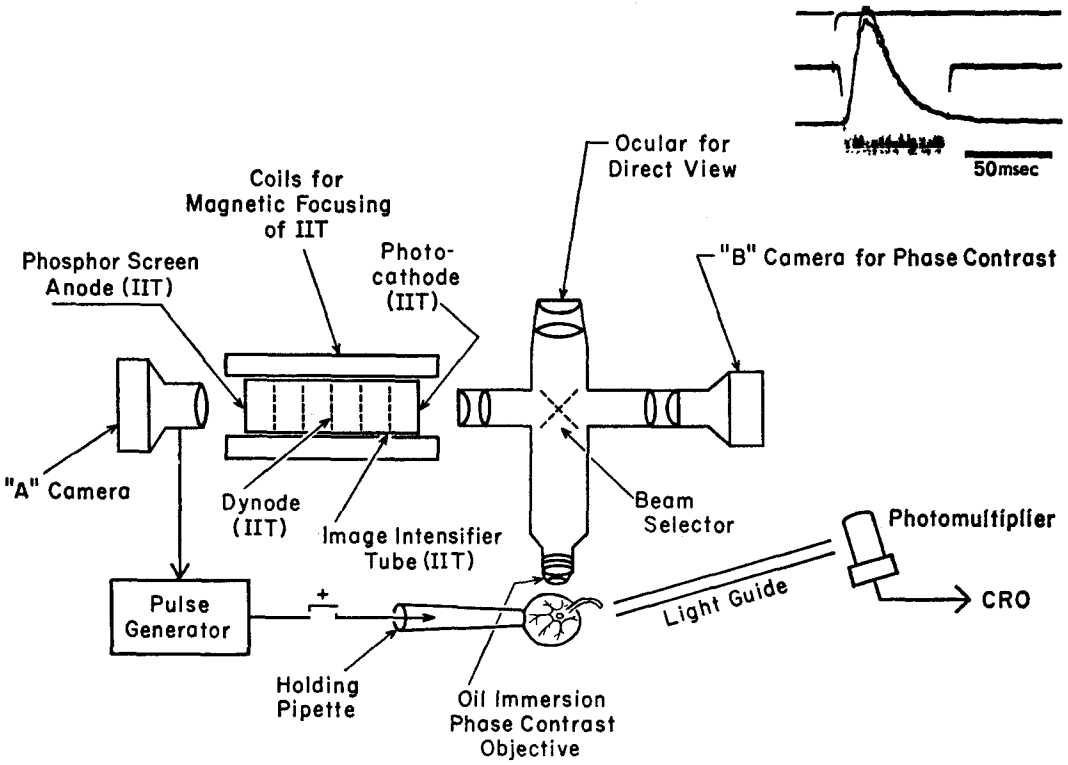

FIGURE 2. Experimental arrangement for autophotography of microsources by image intensification. Specimen was held to stimulating pipette by 2 to 5 mm of water pressure. Pulse generator for evoking the flash was synchronized with "*A*" camera shutter. The photomultiplier signal was displayed on a cathode ray tube in order to permit monitoring of the macroflash. The text gives additional explanation. *Inset* at upper right shows method used to determine synchrony between camera *A* shutter opening and the luminescent flash of the specimen. Upper trace deflection shows stimulus applied to organism; middle trace indicates duration of shutter opening by photometric display of an incandescent source seen by a multiplier tube through the open shutter. Lower trace was obtained with a second photometer, which displayed the time course of macroflash emitted by the stimulated specimen. Two superimposed sweeps are shown.

noise." Its presence necessitated judgements in distinguishing image signal from noise when interpreting autophotographs of microsources. Spots of light due to the various noise sources generally were smaller in diameter than microsource images at the magnifications employed. Some small microsource images, however, may have been mistaken for noise, and may therefore have been overlooked.

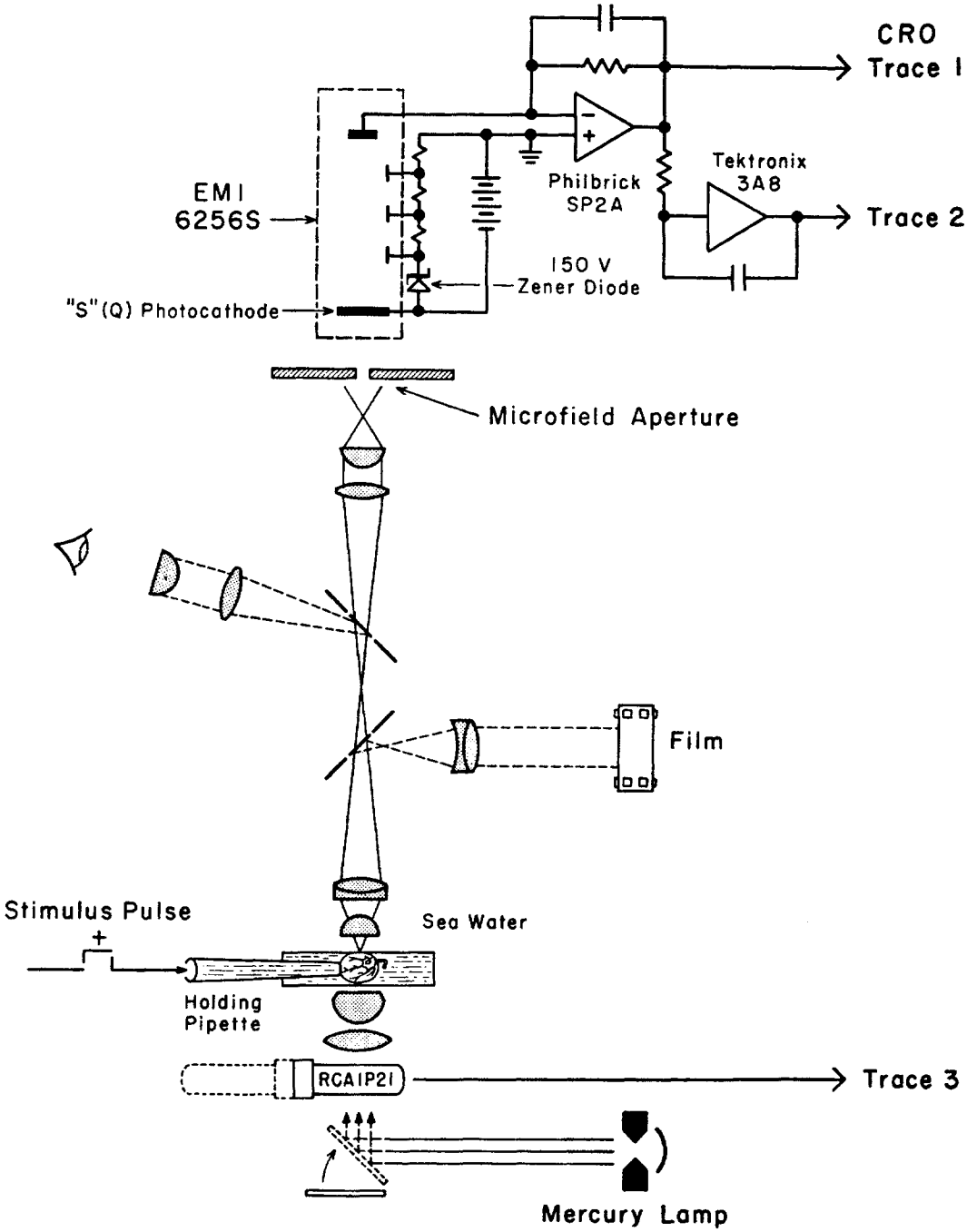

FIGURE 3. Apparatus for concurrent photometry of micro- and macroflash of *Noctiluca*. Regions selected for microphotometry on the basis of phase contrast and fluorescence illumination were brought into the microphotometer field by visual alignment

Autophotographic studies were carried out with the combination of apparatus diagrammed in Fig. 2. The shutter of camera *A*, used to photograph the intensified image, was synchronized with the luminescent flash so as to remain open only for the duration of the flash (Fig. 2, inset) in order to obtain the most favorable signal-noise ratio in the photographed image. Decay time of the image screen phosphor was about 1 msec. Geometric distortions introduced by the intensifier and by the f0.95 lens of camera *A* were determined by photographing the image of a hemocytometer grid at low magnification through the microscope-intensifier-camera *A* axis.

To monitor luminescence during image intensification studies, $\frac{1}{8}$ of an inch diameter glass light conduit was positioned with one end 3 to 5 mm from the specimen and the other end closely directed at the photocathode of an RCA 1P21 multiplier tube. The signal from the photomultiplier was displayed on a cathode ray tube to monitor the approximate magnitude of each flash, and to detect multiple responses, failure to flash, or other anomalies.

Comparisons of autoexposed microsources with structural details of the cytoplasm were carried out by photographing selected areas of cytoplasm both by intensified autoillumination and by phase-contrast illumination. To permit this, the microscope body was fitted with a selector prism which allowed the image of the specimen to be directed either to the photocathode of the image tube, or directly onto the film plane of camera *B* (Fig. 2). Intensified autoilluminated images were photographed from the phosphor screen with camera *A* several seconds after exposure of the phase-contrast image with camera *B*. The image of a hemocytometer grid was used to determine equivalent loci on the camera *A* and camera *B* film planes.

Microphotometric recordings from selected areas of perivacuolar cytoplasm were made with the apparatus diagrammed in Fig. 3. The final pathway of light entering the objective of the Zeiss photomicroscope was selected by means of a prism assembly which directed the image either (*a*) to the observer, (*b*) to the observer and the internal camera, or (*c*) directly to the multiplier tube positioned above the microscope. A calibrated aperture just below the multiplier tube restricted the image falling on the photocathode to a circular area 3 μ in diameter at the level of the specimen. The size of the microfield was established by making the photometer aperture conform with the image of a 120 μ hole (drilled in 0.003 inch brass shim stock) projected to the plane of the aperture through a 2.5 × objective. It was assumed, on the basis of reciprocal proportionality, that the 100 × objective would project a 3.0 μ field through the aperture. The microfield aperture was aligned so that it was optically centered with respect to a cross-hair mounted in one of the eyepieces. The location of the aligned microphotometer field with respect to the format of the microscope camera

---

with an ocular cross-hair. A photomicrograph was then made with the internal camera to record the position of cytoplasmic structures with respect to the photometer field. Finally, the side-window photomultiplier was swung into position below the condenser, and the selector prism of the photomicroscope was repositioned so as to let the image project upward to the photocathode of the refrigerated EMI multiplier. Photometric measurements were displayed with two traces of an oscilloscope and recorded on film. In some experiments the microphotometer signal was integrated and displayed on a third trace. Text gives further detail.

was then determined by photographing a cross-hair slide which had been aligned with the ocular cross-hair.

The alignment of the system was checked photometrically by measuring the relative amount of light passing through the 120 μ calibration hole, the 2.5 × objective, and the microphotometer aperture. With proper alignment, maximum transmission occurred when the image of the calibration hole was centered with the ocular cross-hair; transmission fell off sharply when the centered image of the hole was displaced in any direction. Parallax was negligible.

The photomultiplier which monitored the microfield was an EMI 6256S with an S(Q) photocathode cooled to −40°C to reduce dark noise. It was generally operated at 1700 v, with the anode current monitored by a Philbrick SP2A operational amplifier in a current-to-voltage transimpedance circuit (Sheingold, 1964). A capacitor in parallel with the feedback resistor was used to slow the signal somewhat to avoid "ringing" in the amplifier. About 3% of photons emitted in all directions from an object in the plane of focus of the microphotometer gave rise to photoelectrons in the multiplier, as calculated from the numerical aperture of the objective and the quantum efficiency of the photocathode.

Photometry of light emitted from the entire organism (the macroflash) was carried out concurrently with that from the microfield with an R3A 1P21 side-window multiplier tube (S4 cathode) below the substage condenser. The multiplier could be swung out of the light path when transmitted illumination was required.

Micro- and macrophotometer outputs were displayed on separate traces of a cathode ray tube and photographed. Both photometer systems were DC-coupled and had upper frequency time constants faster than 1 msec. In some experiments the microphotometer signal was integrated by an operational amplifier for display on a third trace. In that application the time constant of the integrating network was 0.01 sec.

When stimulated to flash, the noctilucas also twitch, which tends to displace the region under observation with respect to the optical field. This interfered greatly with the design and execution of certain experiments, especially those involving repetitive responses.

RESULTS

Morphology of the Perivacuolar Cytoplasm

The cytoplasm which comprises the perivacuolar layer has a complex configuration. Although this layer has been conceptually simplified into a sheet for bioelectric considerations (Eckert, 1965 *b*), it is not a simple sheet of constant thickness. Instead, it varies in thickness from a small fraction of a micron, where plasmalemma and vacuolar membrane appear to come together with no intervening cytoplasm, to several microns where strandlike accumulations of cytoplasm occur (unpublished electron micrographs by Dr. H. S. DiStefano). The "strands" are irregular in shape and form an anastomosing pattern when viewed in the light microscope (Fig. 1). They are labile in configuration, slowly rearranging themselves by streaming move-

ments. At numerous points the perivacuolar cytoplasm forms a continuum with the cytoplasmic strands which radiate from the perinuclear mass. The inner (vacuolar) membrane is highly complex in its three dimensional configuration. In addition to forming a continuum, via the radial strands, with the membrane which limits the perinuclear mass, the vacuolar membrane is highly convoluted as it follows the contours of the strandlike thickenings of the perivacuolar cytoplasm.

Phase-contrast microscopy of the perivacuolar cytoplasm revealed little structural detail other than anastomosing strandlike thickenings of the cytoplasm and many dark, *strongly phase-retarding bodies* (SPRB's) ranging in diameter from 1.5 μ to below 0.2 μ (Figs. 1 and 4). Inclusions of generally similar appearance were also observed in specimens of a nonluminescent form of *Noctiluca* (Eckert and Findlay, 1962).

The microsources of luminescence found in *Noctiluca* are confined very largely to the perivacuolar cytoplasm. While they have not yet been recognized in electron micrographs, they have been identified by both fluorescence and phase-contrast microscopy, as described below.

Fluorescence of Microsources

Since it is known that firefly luciferin fluoresces (Strehler and McElroy, 1949), specimens of *Noctiluca* were examined with ultraviolet illumination to determine whether fluorescence might serve as a method for identification of microsources. Upon illumination with the 365 and 404 mμ lines, numerous sources of fluorescence were observed within the perivacuolar cytoplasm (Fig. 4, A_1). Graded introduction of tungsten phase-contrast illumination during ultraviolet excitation revealed that the observed fluorescence invariably originated in certain of the round phase-retarding bodies (SPRB's) (Fig. 4). 5000 μ^2 areas from each of six specimens were photographed and counted to determine the numbers of fluorescent sources, as well as the total number of SPRB's (Table I). Considerable variability was found, but on the basis of these counts representative numbers for a 500 μ diameter specimen were calculated to be of the order of 10^5 SPRB's, of which 1 to 5×10^4 were fluorescent. No other fluorescence was detected in *Noctiluca*, other than a red emission from ingested chlorophyll-bearing algae.

Whereas initial microscopical observations failed to detect distinct morphological classes among the population of SPRB's, the discovery of fluorescence in part of this population prompted a more critical examination. It was subsequently noted in tungsten phase-contrast illumination that the fluorescent inclusions generally show a smaller degree of phase retardation (they appear slightly lighter in positive phase contrast) than the nonfluorescent members of the SPRB population (Fig. 4). Moreover, they exhibit a larger range of diameters, some larger and others smaller than any of the nonfluorescent bodies. Fluorescent organelles range in size from about 1.5 μ in

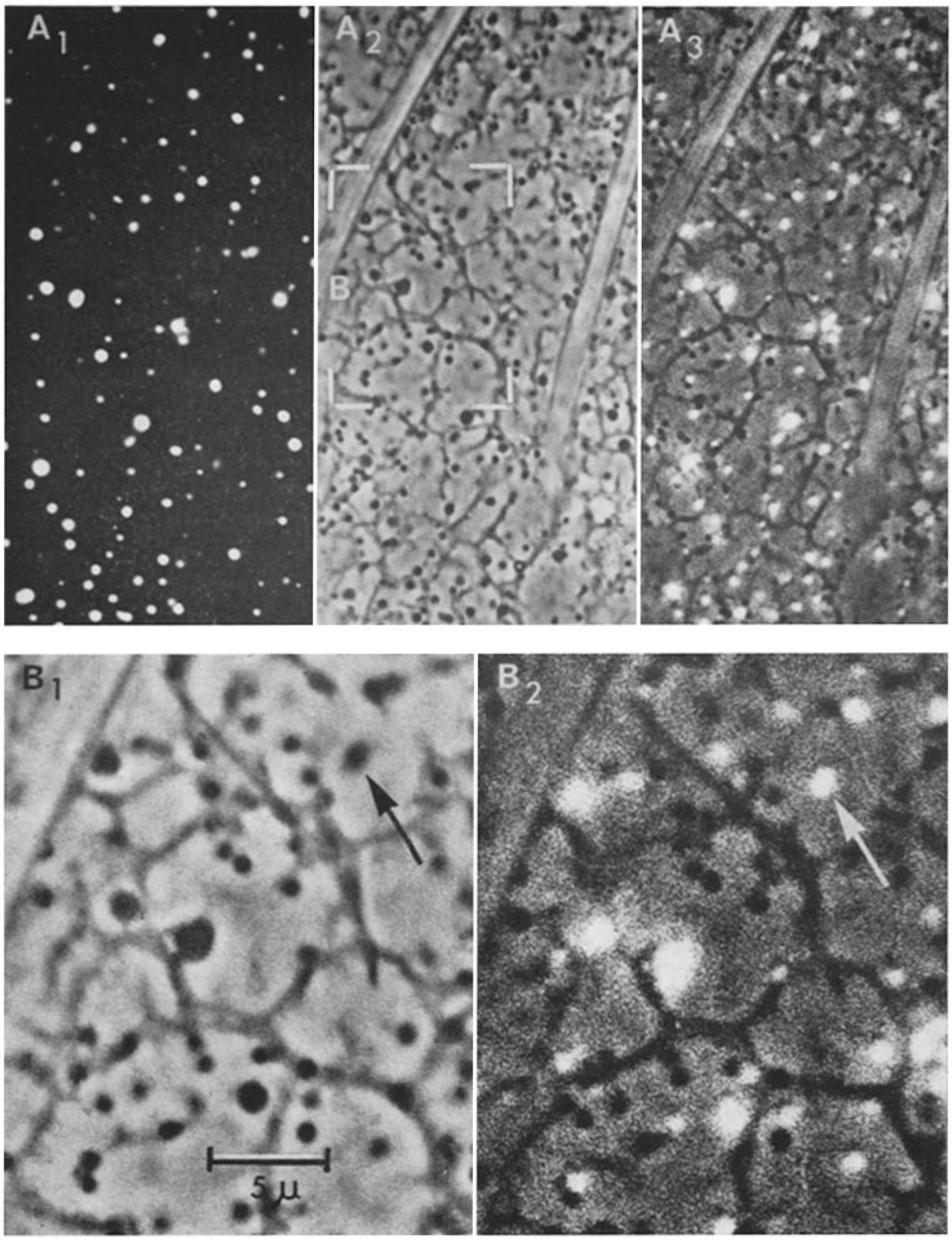

FIGURE 4. Fluorescent bodies in the perivacuolar cytoplasm of *Noctiluca*. A_1, photomicrograph of a 32 × 63 μ field showing fluorescent sources; A_2, same field by phase contrast showing SPRB's, and strandlike cytoplasmic thickenings. A_3, same field by phase contrast/fluorescence illumination (see text). Large diagonal structures in A_2 and A_3 are folds in the pellicle. B_1 and B_2 show details of the area outlined in A_2. Comparison of the phase contrast with the phase contrast/fluorescence image will indicate which of the SPRB's in B_1 were fluorescent (e.g., arrows).

diameter to less than 0.2 μ. The evidence indicates a clear dichotomy between fluorescent and nonfluorescent SPRB's, for no gradations in degree of fluorescence other than those due to variations in microsource size were noted within individual specimens. The identity and function of the nonfluorescent organelles of the SPRB population are not known.

Evidence that the fluorescent bodies are identical with the microsources of luminescence came initially from direct microscopic observation. The SPRB's which fluoresced during ultraviolet excitation brightened perceptibly to the observer's eye when the specimen was stimulated to flash during observation of the fluorescing bodies. We also noted an absence of fluorescent organelles

TABLE I

NUMBERS OF FLUORESCENT ORGANELLES PER CELL

5000 μ^2 areas of perivacuolar cytoplasm were photographed by phase contrast, fluorescence, and phase contrast/fluorescence illumination (see Fig. 4) in five specimens of *Noctiluca*. The total number of SPRB's and the number of those which showed fluorescence were counted in each field. The figures were normalized for the surface area of a sphere of 500 μ diameter, which approximates the perivacuolar area of a *Noctiluca* specimen of typical dimensions. The numbers listed are therefore extrapolated approximations.

Specimen	Normalized No. of SPRB's $\times 10^4$	Normalized No. of fluorescent bodies $\times 10^4$	$\frac{\text{Fluorescent bodies} \times 100}{\text{All SPRB's}}$
A	8.9	1.4	16
B	13.0	4.5	35
C	12.0	3.0	25
D	11.0	5.3	48
E	7.1	4.8	68
F	11.0	3.0	27
Mean $\pm$SD	10.5$\pm$2.0	3.6$\pm$1.7	36$\pm$17

in the nonluminescent population of *Noctiluca* obtained from Puget Sound (Eckert and Findlay, 1962). Final evidence equating the microsources with the fluorescent SPRB's is given below in the section on photometric experiments.

The color of the fluorescence, as observed through a barrier filter with a 525 mμ low wavelength cutoff, was green, and was therefore consistent with the spectral composition of the luminescence which peaks at about 470 mμ and extends beyond 540 mμ (Nicol, 1958).

Dimensions of Microsources

It had been noted during visual examination that microsources exhibit a range of diameters below 1.5 μ (Eckert, 1966 *a*), and that in some cells the mean diameter deviates somewhat from the norm. The combination of fluorescence and phase contrast in the same image has permitted a more critical examina-

tion of the size distribution of microsources by photographic means. Photomicrographs similar to those of Fig. 4 were made of areas of 4000 μ^2. Microsources were identified in the phase-contrast photos by comparison with the combination phase-contrast/fluorescence photos and were circled with ink. The phase-contrast photographs were then enlarged 10 diameters by an

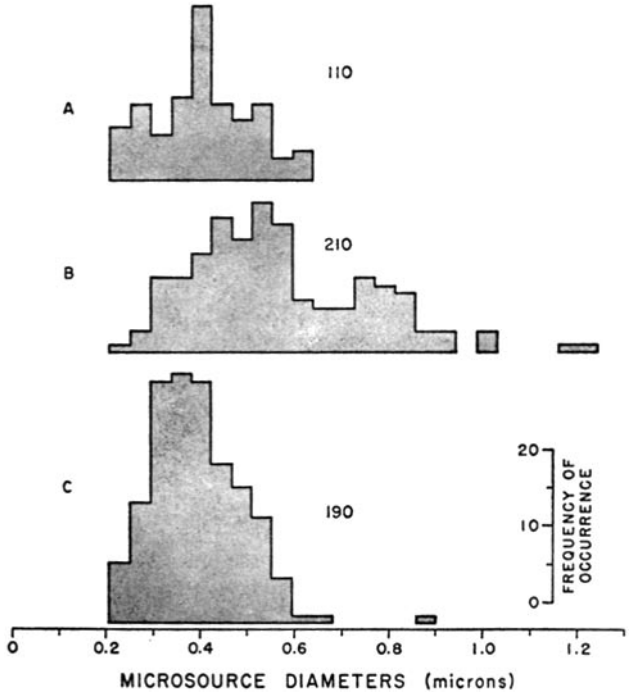

FIGURE 5. Size distributions of microsources in three specimens of *Noctiluca*. Microsources were identified by phase contrast/fluorescence (Fig. 4) and measured, and size distributions were plotted as histograms. *A*, *B*, and *C* represent distributions of three specimens. The numbers adjacent to each histogram represent the number of microsources measured within a 4000 μ^2 field. Microsources which could not be positively identified in phase contrast were ignored and did not enter into these tabulations. Some microsources were too small to be measured, hence, size distributions extend lower than indicated. The method of measurement is described in the text.

opaque projector, and microsources were individually measured with calipers. Fig. 5 shows histograms of size distributions in three specimens.

No discontinuities in size distribution are evident with phase-contrast optics. However, accuracy of measurement was limited by optical resolution. For this reason, also, the lower limit of microsource diameter is assumed to extend below those shown by the histograms. According to these measurements, the most common diameters lie around 0.4 μ. Histogram *B* was made from the cell used for Fig. 4. It had especially large, strongly fluorescent microsources, and therefore served well for photographic purposes.

The small size of the organelles renders their true shape difficult to determine by light microscopy. If it is assumed that they are nearly spherical, a range in diameter of 0.2–1.0 μ represents a surface ratio of 25 and a volume ratio of 125. A quantitative correlation of microsource dimensions with emission strength has not yet been made.

The perivacuolar cytoplasm was examined with the help of Dr. Hidemi Sato with Professor Inoué's rectified polarizing microscope, but did not exhibit any highly birefringent bodies similar to those observed in *Gonyaulax* (Hastings et al., 1966).

Autophotography of Microsources

Certain functional characteristics of microsources can be examined best with the aid of photomicrographs exposed by the emitted light. Attempts at direct autophotography failed, because the light emitted was insufficient for even the fastest available film. Indirect autophotography was made possible, however, by the technique of image intensification (Reynolds, 1964; Eckert, Reynolds, and Chaffee, 1965). Fig. 6 shows low power autoilluminated photomicrographs of whole organisms which were obtained by this technique.

The distribution of microsources within the perivacuolar cytoplasm was examined by the comparison of phase-contrast micrographs with autophotographs of microsources in the same field exposed several seconds later by their electronically intensified emissions. Relative displacements due to slow streaming movements of the cytoplasm made it difficult to unequivocally locate microsources with respect to the phase-contrast image. The results do indicate, however, that the emissions are associated with some of the phase-retarding inclusions (Fig. 7), and thereby lend support to similar evidence from fluorescence and photometric studies. Additional evidence for the origin of light emission in the SPRB's was obtained by autophotography of microflashes at three levels of microscope focus. Fig. 8 demonstrates that the microsource images were in the best focus when the microscope was focused in the plane of the phase-retarding organelles.

In order to determine, by autophotography, the approximate number of microsources in a specimen, counts were made of autophotographed microflashes in areas of 400 μ^2. Table II lists the number of microsources calculated from autophotographs of six specimens. On the basis of these counts an average figure of 1.6 (SD $\pm$ 0.5) $\times$ 10^4 microsources was calculated for a typical 500 μ cell. The figure determined by fluorescence microscopy was 3.6 $\times$ 10^4 ($\pm$1.7) per 500 μ cell (Table I). There was large variation in the abundance of microsources in specimens from different culture dishes, a reflection, perhaps, of differing states of nutrition or cell cycle. However, the discrepancy could have been due in part to confusion of the smaller microflash signals with image noise in interpreting autophotographs obtained with

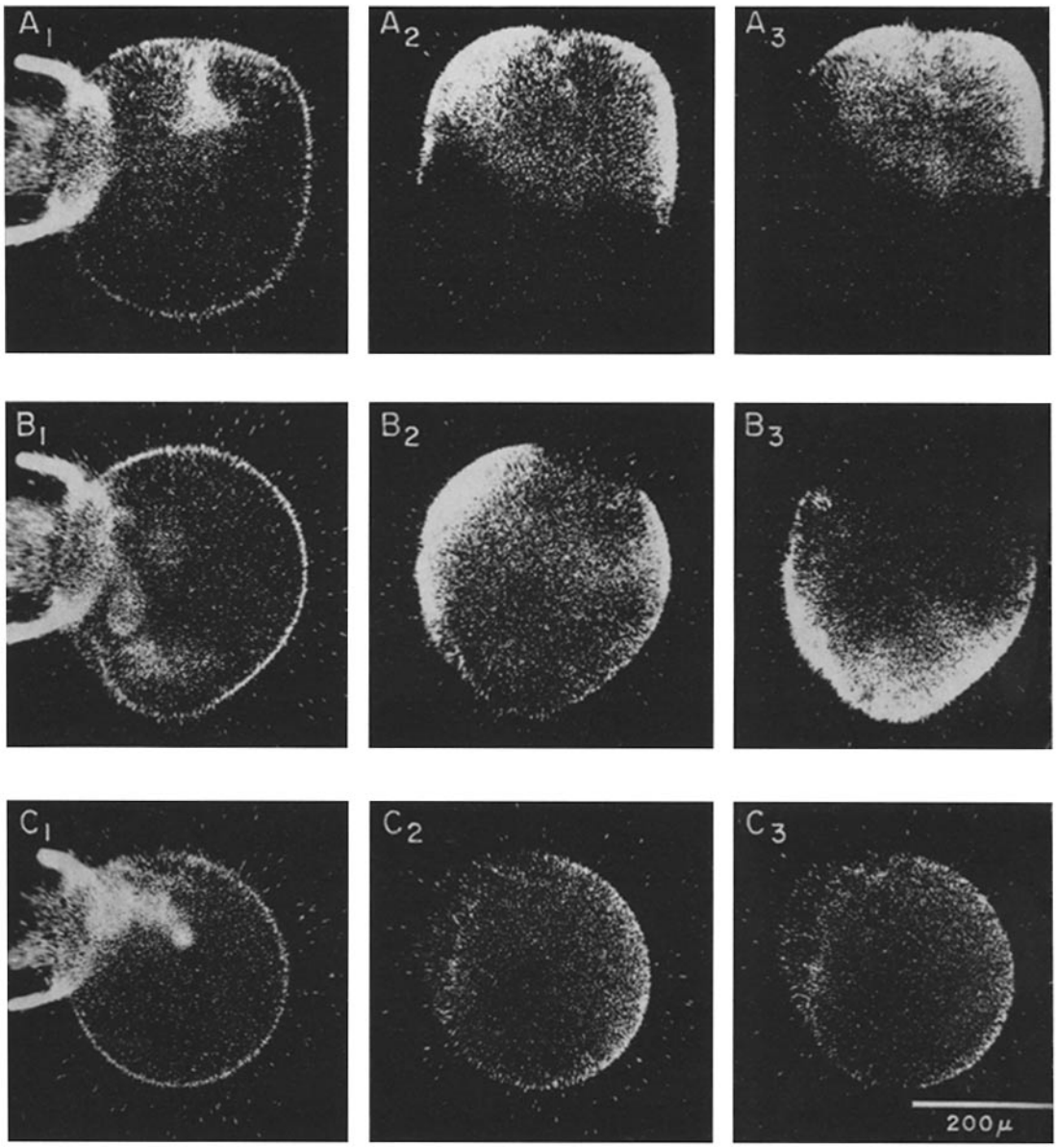

FIGURE 6. Intensified images of *Noctiluca* by emitted light. A_1, B_1, and C_1 were obtained by low gain intensification of specimens by dark-field illumination. Object at left is end of holding pipette. A_2, B_2, and C_2 show images of the same cells flashing, and were obtained by electronic image intensification as described in the text. A_3, B_3, and C_3 were obtained several minutes later. Incomplete images in series A and B were the result of failure of emission from portions of the cell, rather than asynchrony of camera shutter with flash (see Fig. 2, inset). Specimen C continued to exhibit emission from all regions of the cell. Spots outside of cell are noise (see text). Graininess of image is primarily due to graininess of intensification.

intensification. Therefore, the higher figure $(3.6 \pm 1.7) \times 10^4$ is considered the more reliable value for the number of microsources contained in a typical specimen 500 μ in diameter.

Average Number of Photons Emitted by Microsources

The emission which constitutes the macroflash of an unfatigued cell of about 500 μ diameter contains of the order of 2 to 5 $\times$ 10^9 photons (Eckert, 1965 *a*, footnote 1). Dividing by the number of microsources (a mean of 3.6×10^4,

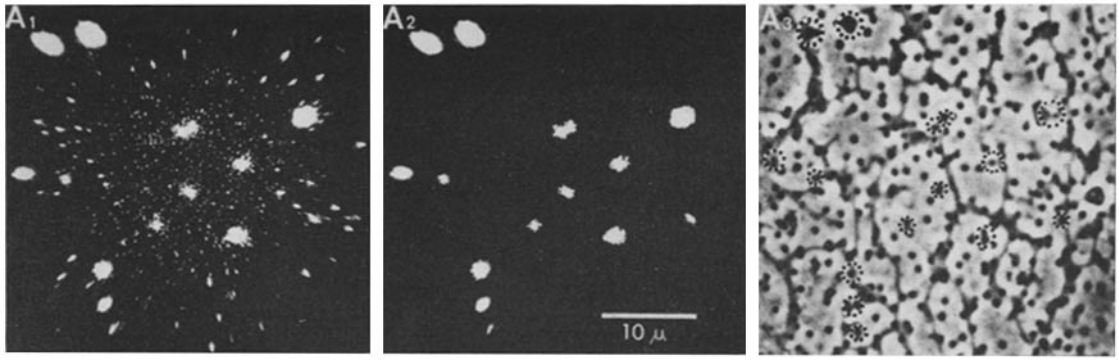

FIGURE 7. Spatial comparison of autophotographed microsources with SPRB's. A_1, photograph of image formed by image intensifier tube of a field 40 μ in diameter. Auto-illumination of microsources came from a single response by specimen, so that each microsource was exposed by the intensified image of its microflash. Most of the scattered fine spots are due to diffuse background light or to noise inherent in the image tube. Small spots, which include noise and possibly some small microsources, were inked out in A_2 in order to present an unequivocal picture of the major microsources in that field. A_3 shows a phase-contrast image taken of the same field several seconds before A_1. Superimposed on the phase image are dotted circles to indicate location of microsources. These were transposed from A_1 *after* correction for distortions introduced by the image tube. Note the spatial correlation of microsources with some of the SPRB's (from Eckert, 1966 *c*).

as determined by fluorescence photomicrography) yields a figure for omnidirectional "unfatigued" microsource emission of the order of 10^5 photons per microflash. Because of the large range in microsource size and emission strength (Figs. 4, 5, 9, and 12), individual microflashes must deviate considerably from this calculated mean. The validity of the calculation rests on the apparently normal size distribution of microsources (Fig. 5), and on evidence (presented in the next section) that a microsource normally contributes to each macroflash.

A more direct determination of the number of photons per microflash was

[1] Eckert, R. 1967. The wave form of luminescence emitted by *Noctiluca J. Gen. Physiol.* (in press).

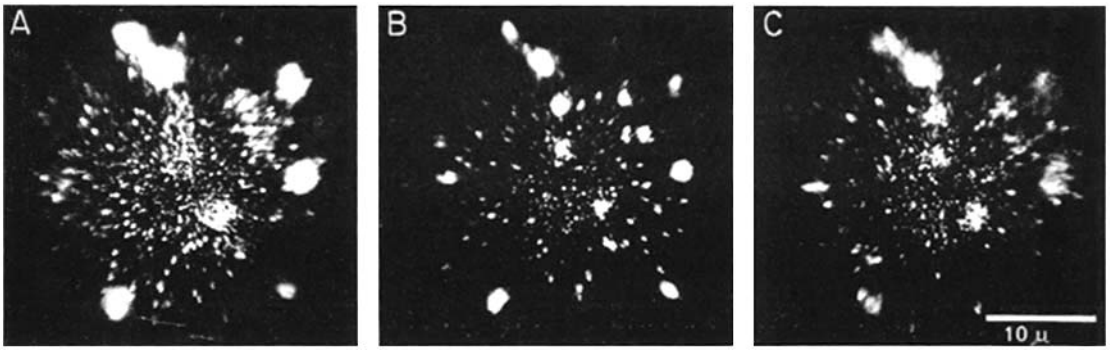

FIGURE 8. Autophotographs of microsources at three levels of focus. *A*, focus plane 1 to 2 μ above SPRB's in perivacuolar cytoplasm. *B*, focus plane at level of phase-retarding bodies. *C*, focus plane 1 to 2 μ below level of SPRB's. Note differences in degree of focus of autophotographed microsources. Time elapsed between exposures was about 1 min.

TABLE II

NUMBERS OF MICROSOURCES PER CELL AS DETERMINED BY IMAGE INTENSIFICATION

Identical 400 μ^2 areas from paired photographs of the phase contrast illuminated and of intensified autoilluminated fields were counted to give numbers of all SPRB's, and numbers of autoexposed microsources. These numbers were normalized for the area of a sphere 500 μ in diameter, which approximates the area of the perivacuolar cytoplasm of a typical specimen. The figures listed are therefore extrapolated approximations.

Specimen	Normalized No. of SPRB's × 10^5	Normalized No. of microsources × 10^4	$\frac{\text{Microsources} \times 100}{\text{All SPRB's}}$
I	3.7	1.6	4.3
II	2.4	1.3	5.4
III	2.7	1.0	4.0
IV	2.5	1.8	7.2
V	2.0	2.6	13.0
VI	2.2	1.3	5.9
Mean ±SD	2.6±0.6	1.6±0.5	6.3±3.0

made in conjunction with image intensification. The photograph of a flash obtained from the output phosphor of the intensifier shows an individual microsource in the field of view as an exposed region on the film of the order of 1 mm in extent. Within this spot there is a pattern of film grains rendered developable by the light from the source which was intensified by the tube. A known fraction f_m of the photons emitted from the source is accepted and transmitted by the microscope system to the cathode of the image tube.

Photons striking the cathode cause electrons to be emitted from the cathode with a known efficiency E_c. Each of these electrons is accelerated and multiplied in the dynode structure of the image tube so that for each initial photoelectron a bundle of electrons strikes the anode (output phosphor) of the tube and causes an intense spot of light which is about 40 μ in diameter. The intensities of the spots of light due to individual electrons vary significantly in the type of tube used in the present investigations (Reynolds 1966 *b*), and

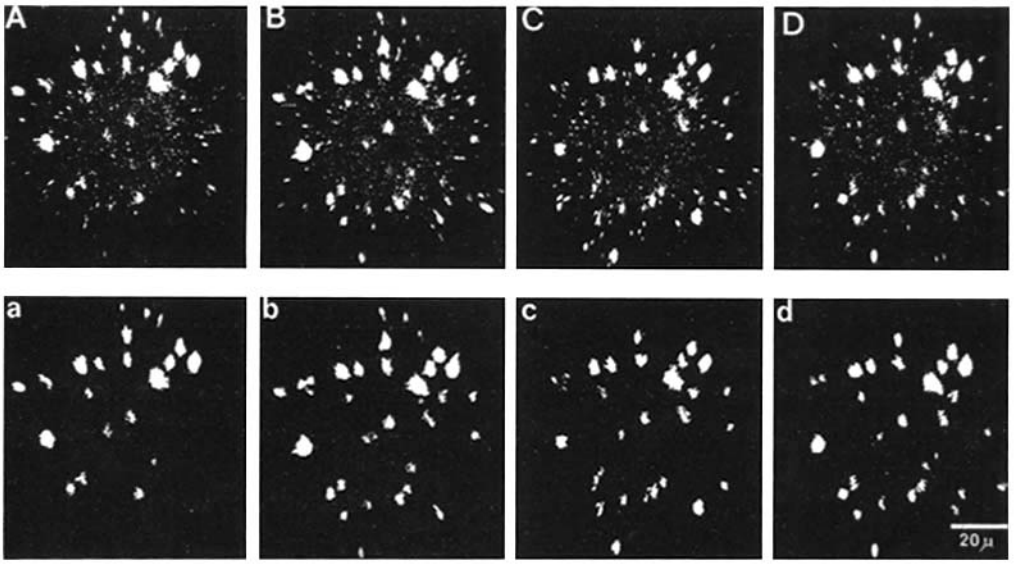

FIGURE 9. Consistent recurrence of microsource emissions. *A–D*, four intensified images of a single microscopic field taken at about 1 min intervals. *a–d*, same photographs with noise and equivocal signals (those readily confused with noise) inked out. Changes in the pattern of microsources between *a* and *b* are due to relative displacements within the cytoplasm. Note the recurrence of microsource responses with repeated stimulation of the organism.

the gain of the tube refers to the average intensity of the spots. The spots can be detected on the film with an efficiency E_e which tends to be low in spite of the high gain of the tube because of the fluctuations referred to above. The average number of spots, $\bar{N}_e$:, counted in the region of film corresponding to a microsource thus allows a calculation of the average number of photons emitted by the microsource, $\bar{N}_{\nu 1}$

$$\bar{N}_{\nu 1} = \frac{\bar{N}_e}{\bar{E}_e} \cdot \frac{1}{\bar{E}_c} \cdot \frac{1}{\bar{f}_m}$$

Measured values for the quantities were:

$E_e = 0.15 \pm 0.05$ (Reynolds and Botos, 1965; Reynolds 1966 *a*)

$E_c = 0.104 \pm 0.010$ (Reynolds and Botos, 1965)

$f_m = 0.097$ (based on values provided by Carl Zeiss, Inc.)

$\bar{N}_e$ was determined for 36 different microsources, exhibiting a variation in photon output of 8:1. The mean of these determinations was 80. Thus:

$$\bar{N}_{\nu 1} = (5.3 \pm 3.0) \times 10^4 = \text{average number of photons emitted.}$$

A second method of determining the number of photons emitted by a microsource is based on the fact that the average number of photons, n, required to cause the development of each of the grains in the microsource image has been determined (Reynolds and Botos, 1965; Reynolds, 1966 *a*). The number of grains, Ng, developed in the image of each source can be measured by a densitometer technique, calibrated for the films used and corrected for film background. Thus, if f_c is the fraction of photons given off by the intensifier phosphor that is transmitted to the film by the camera lens, and G is the gain of the image tube (defined as the ratio of the average number of photons emitted at the anode to the number of photons incident on the cathode), then the number of photons emitted by the microsource, $N_{\nu 2}$, is given by:

$$N_{\nu 2} = \frac{N_g \cdot n}{f_c G} \cdot \frac{1}{f_m}$$

Measured values were:

$n = 220 \pm 20$ (Reynolds and Botos, 1965; Reynolds 1966 *a*).
$f_c = 0.05 \pm 0.005$
$G = (8.0 \pm 1.0) \times 10^5$
$\bar{N}_g = 5.65 \times 10^5$
$f_m = 0.097$

Ng was determined for 16 different microsources, with a variation in photon output of 5:1. Thus:

$$\bar{N}_{\nu 2} = (3.2 \pm 1.0) \times 10^4$$

The two methods are, of course, related in principle and must be consistent with each other. In view of the spread in the number of photons corresponding to each cathode electron (Reynolds 1966, *b*) and in view of the independence of the measurements involved, it is useful in practice to utilize both.

The final value for the average number of photons per flash for the microsources measured is $(4.4 \pm 1.5) \times 10^4$.

The uncertainties given above for E_e, E_c, f_c, n, and G make the absolute value for $\bar{N}_\nu$ correspondingly uncertain. However, in the measurements of the changes in individual microsource emission in a time sequence of responses to be discussed below, *relative* photon outputs are not correspondingly uncertain, since the same values of G, E_e, f_c, etc., whatever they were, applied to all the observations in the sequence.

The mean photon content of the microflash (1.4×10^5) calculated by dividing the mean unfatigued macroflash emission by the average number of sources is three times as great as the value (4.4×10^4) calculated from the image intensifier data. These two independently obtained values for the quantum content of the microflash are, however, in relatively good agreement, for the variability in photon content of macroflashes recorded among specimens varies over a range of two orders of magnitude.[1]

The Basis of Macroflash Intensity Gradations

Reversible, graded changes in macroflash amplitude (i.e., summation, potentiation, fatigue) normally occur as functions of flash interval (Eckert, 1965 *a*, Fig. 3; footnote 1). These changes in emission strength could have as their basis either one or both of the following alternatives. (*a*) The number of *reactive* microsources could change, an increase in the number of emitting organelles resulting in a larger macroflash, and a decrease in the number of reactive microsources resulting in a smaller macroflash. (*b*) The amount of light produced by the individual microsources of a numerically stable reactive population could increase or decrease, and thereby alter the amplitude of the macroflash.

The reactive stability of microsources was tested by experiments such as that illustrated in Fig. 9. The reproducibility of microsource constellations as seen in this sequence, and in all others of similar experiments, is taken as evidence that individual microsources flash in response to each flash-triggering action potential. According to this interpretation, each macroflash in a series of responses arises from a numerically stable population of reactive microsources. This eliminates the alternate possibility; namely, that with each response of the cell a labile fraction of the total microsource population is activated.

Although all the microsources observed within a small area of the perivacuolar cytoplasm appear to respond as an all-or-none group, the entire population of microsources contained in large areas of cytoplasm sometimes ceases to respond while the rest of the cell continues to flash (Fig. 6, series *A* and *B*). Luminescence from the whole perivacuolar cytoplasm (Fig. 6, series *C*) was the normal response in fresh preparations. It seems likely that the

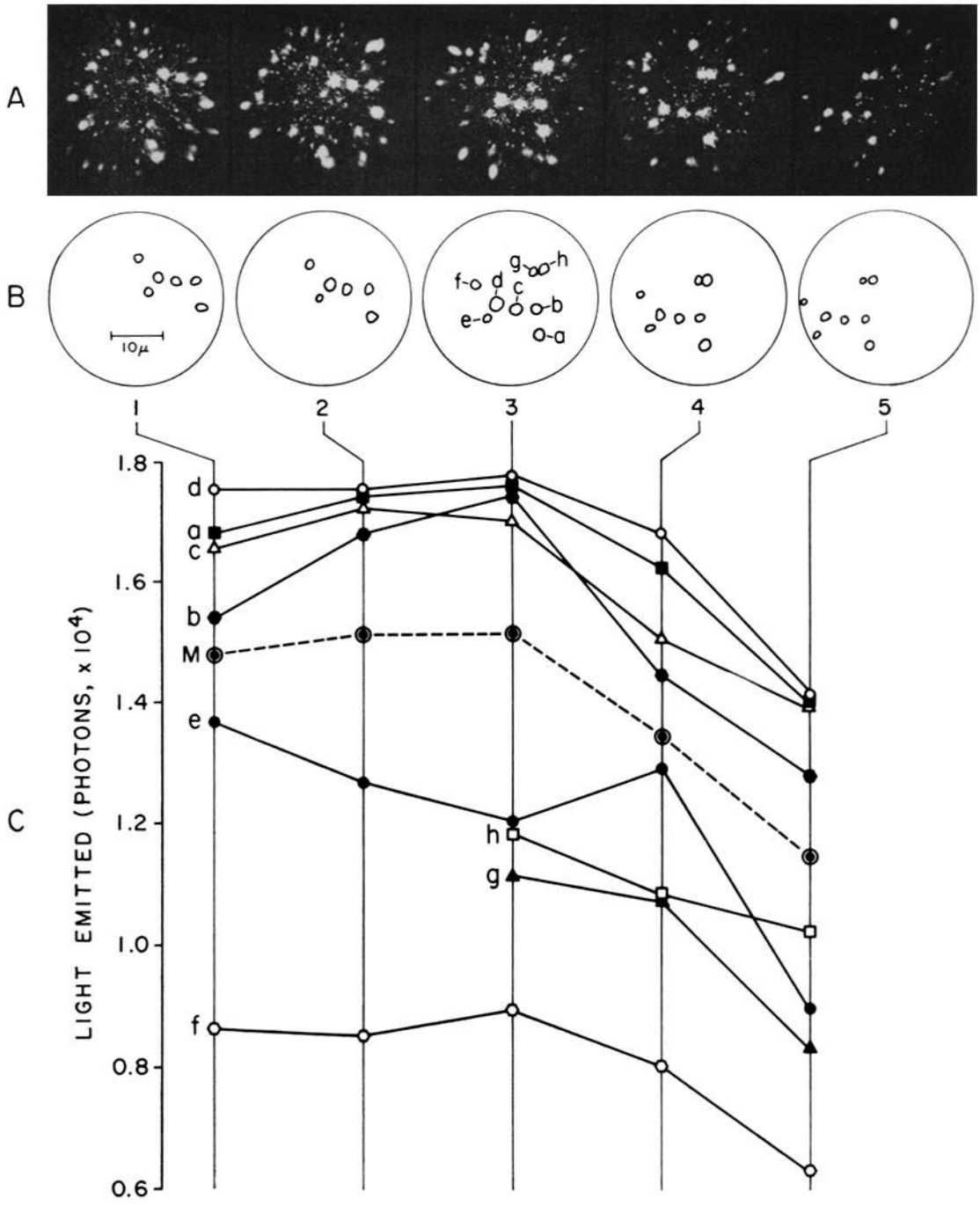

FIGURE 10. Changes in individual microsource emission strength in a sequence of responses. *A*, consecutive sequence of images, obtained from the image tube, showing microsources exposed by their intensified emissions. Intervals between frames were not

rapid and irreversible decrease in peak intensity of the macroflash exhibited by certain specimens during a sequence of stimulations is the result of a regional failure of propagation of the flash-triggering potential. Local failure of the action potential has been noted by surface recording in unpublished experiments. It is evidenced by a graded decrease in and final loss of the positive-going spike of the triphasic action potential recorded from the surface, and a retention of the negative-going passive component. No attempts have yet been made to directly correlate local conduction failure with regional failure of luminescence. The failure of portions of the cell to flash is to be distinguished from fatigue of the flash, which is the reversible decrease in amplitude that results from a reduction in the interval between stimuli.[1]

The second alternative mechanism, namely, that reversible gradations in macroflash amplitude result from gradations in individual microsource emissions, was tested by measuring the intensity of microsource images in a sequence of flashes which underwent intensity changes. The object was to determine whether individual microsources show graded changes in the amount of light emitted from one response to another, and, if so, to determine whether they do so proportionally with one another, or with large degrees of freedom.

Fig. 10 shows a consecutive sequence of intensified images of an area of cytoplasm about 40 μ in diameter. This sequence was selected for analysis because it contained several microsources which remained within the field for several frames, and which underwent significant changes in emission strength during the series of responses. A densitometer technique (see previous section) was utilized to determine the photon outputs represented by the individual microsource images. The values obtained were plotted to show variations in emission strength of individual microsources in the five-flash sequence (Fig. 10 *C*). Inspection both of the images and the graph reveals that the microsources underwent changes in emission strength and that they did so ap-

---

of uniform duration, but ranged around 30 sec. Photographic reproduction was controlled to retain relative values of intensity; however, contrast was somewhat enhanced over that of the negative. The progressive displacement of the microsource constellation resulted from movements of the cell in response to stimulation. *B*, tracings of microsource images (*a–h*) whose exposure intensities measured from the negative are graphed in *C*. *C*, light production by individual microsources indicated for each of the five successive flashes. The ordinate refers to omnidirectional emission. Connected points represent the five successive photon emissions of one microsource. Points connected by dashed line (*M*) indicate means of sources *a–f*. Microsources *g* and *h* were measurable with reliability in frames 3–5 only.

Microsource images very close to the edge of the field (i.e., source *b*, frame 1) were badly distorted and reduced in apparent intensity. Otherwise, the measurements of exposure intensity have an estimated maximum relative error of 0.15×10^4 photons, due primarily to unevenness of the background.

proximately parallel with one another. Such correlations between microsource exposures were noted in every sequence which showed noticeable intensity changes, and in which the same microsources were retained in several frames. In those sequences in which aggregate intensity changes were minimal (e.g., Fig. 9) there was little variation from frame to frame in the intensity of individual microsource images.

Because of the unavoidable and uneven contribution of image noise to the intensity of microsource exposures, the relative error of the points plotted in Fig. 10 *C* is uncertain, but may be as great as 0.15×10^4 photons. Since the plotted deviations from proportionality of microsource images lie within this

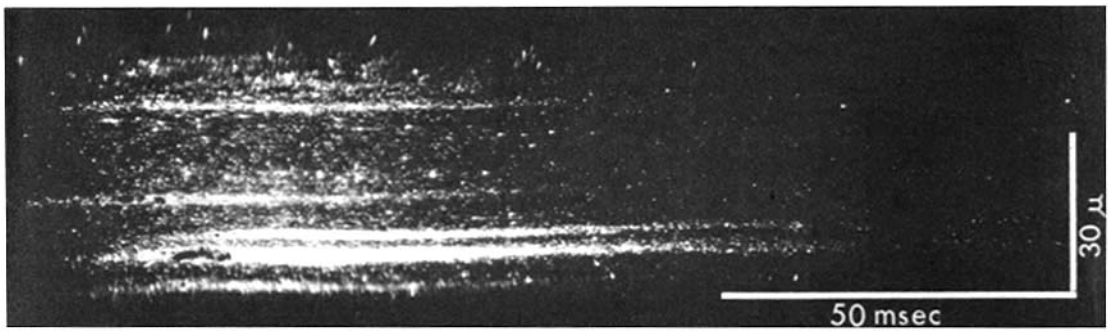

FIGURE 11. Time course of microsource emission examined with kymograph photography. A field 20 μ wide was exposed to moving film during a flash, giving rise to longitudinally smeared images of the microsource emissions. Emissions are seen to trail off somewhat more gradually than they begin. The emissions shown here are atypically strong; most other attempts resulted in grossly underexposed negatives. Vertical perturbations in the streaks are due to slight movement of the specimen in response to stimulation.

range, it is uncertain whether rigid proportionality between microsource emissions was maintained. Even if strict proportionality is not maintained, it is evident that the emissions from neighboring microsurces undergo sequential changes which are at least approximately in parallel.

The dimension of time was added to autophotography by continuous linear movement of the recording film during exposure of microsurces. A Grass C4 kymograph camera was used to move 35 mm film past a 50 mm f0.95 lens at a rate of 1 meter per sec. The field was masked so that at any instant a segment of film 1 cm long was exposed to the anode of the image tube. No shutter was employed. The specimen was stimulated to flash during the movement of the film so as to smear the intensified microflashes along the length of the film (Fig. 11). This technique provided the first evidence that each microflash, instead of occurring as an intense, brief scintillation, has a

time course comparable in duration to that of the macroflash, and similar to those of microflashes arising from neighboring organelles. This was confirmed by photometric measurements described in the following section.

Photometric Measurements from Single Microsources

Intensity-time curves of microflashes were obtained by photometric recording from single microsources in the intact cell. The apparatus (Fig. 3) permitted concurrent monitoring of both the macroflash and microflash to permit comparison of the signal recorded from the microfield with that recorded from the whole cell.

Photometric recordings were obtained from areas of the perivacuolar cytoplasm 3.0 μ in diameter. After alignment of a selected structure within the microfield, and photographic documentation of its position by the internal microscope camera, all lights were extinguished, and a flash was elicited by stimulating the cell with a 1.0 msec pulse of current delivered through the suction pipette which held the cell. Because of cellular movement which occurred with each stimulus, it was nearly always necessary to reposition the image within the microfield prior to each subsequent recording. When the organism flashed, a photosignal was always recorded, regardless of the location of the microfield with respect to cytoplasmic structures. When no fluorescent bodies were aligned with the field of the microphotometer, a minimal signal was recorded (e.g., Figs. 12 *A*, *E*; 13 *A*; 14 A_1, B_1, D_1, E_1). This basal signal is interpreted as a background emission arising primarily from sources included within the field of the microphotometer, but present in the perivacuolar cytoplasm on the far side of the cell, several hundred microns below the plane of focus. To a far lesser degree, this signal may have included scattered light originating from microsources in the plane of focus but external to the microphotometer field.

Although photometric recordings were made from numerous cytoplasmic loci, luminescence exceeding background levels was recorded only from inclusions which exhibited fluorescence. After this relationship had been repeatedly confirmed, microsources were identified for recording purposes by their fluorescence. A consistent correlation existed between the size of a fluorescent inclusion and the amount of light contained in its microflash. Fig. 12 shows microphotometer recordings taken from sources of three widely different sizes. Before the photosignal was displayed and photographed, the approximate diameter of the fluorescent microsource positioned within the microfield was estimated and noted in writing. The examples shown are two representative series of frames. Electronic integration (trace 2) of the microphotometer signal (trace 1) gave relative values for total flux recorded from the microfield during the period of integration. Failure of "small" sources to add significantly to background signal was probably due to the large ratio

(circa 40:1) of microfield area to the area of the microsource image; for "large" sources this ratio was as low as approximately 4:1. Except for amplitude differences, signals from microsources of different sizes appeared to be similar.

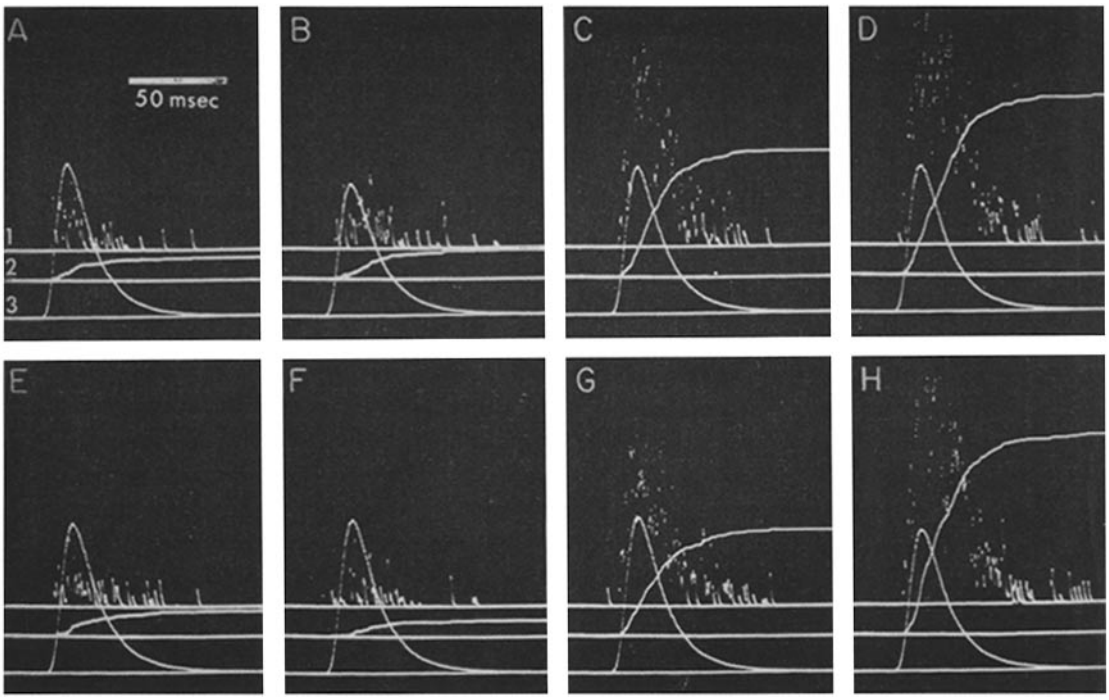

FIGURE 12. Intensity correlation between fluorescence and luminescence of microsources. *Trace 1*, microphotometer signal; *trace 2*, same after electronic integration; *trace 3*, macrophotometer signal. See Fig. 3 for apparatus. *A*, *E*, no fluorescent object in microphotometer recording field; *B*, *F*, small (<0.5 μ diameter) fluorescent source within microfield; *C*, *G*, medium (circa 1 μ) fluorescent source; *D*, *H*, large (circa 1.3 μ) fluorescent source in microfield. Since microsource diameters were estimates, no quantitative interpretations can be made. Note, however: (*a*) relative constancy of macroflash amplitude throughout series; and (*b*) correlation between approximate size of fluorescent organelle and both peak intensity and relative quantum content of the corresponding microflash.

Fig. 13 shows a pair of photometer recordings from two loci within a 17 $\times$ 25 micron field. It demonstrates the method of procedure employed in these experiments. The two adjacent SPRB's at the center of the field exhibited the strongest fluorescence of any structures within the field of the photograph and were also the strongest sources of luminescence. A strong signal was repeatedly obtained from this locus, whereas a sampling of 10 nonfluorescent,

or weakly fluorescent regions in the same field yielded only minimal signals similar to that shown in *A*. The flashes emitted by this prominent pair of microsources (recording *B*) were indistinguishable in time course from those of single microsources (Fig. 14).

As stated earlier, only about 3% of the photons emitted from a microsource gave rise to photoelectrons in the multiplier of the photometer. The relatively low information content of the signal makes accurate wave form interpretations difficult. However, visual inspection of numerous recordings like those

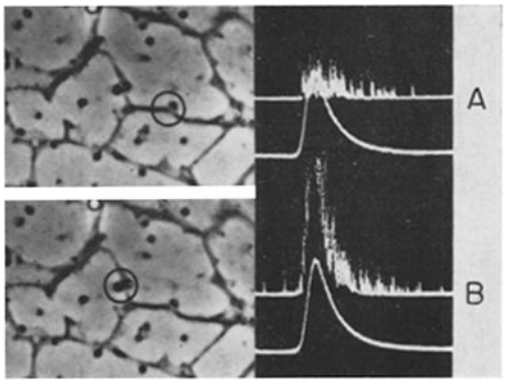

FIGURE 13. Photometric signals from two selected areas in the perivacuolar cytoplasm. To the left of each recording is a phase-contrast photomicrograph with a 3 μ circle to indicate the location (± 1 μ) and size of the area monitored by the microfield photomultiplier. *Upper trace* of each CRO sweep shows the microphotometer signal. Brief deflections of this trace represent single photons or groups of closely spaced photons impinging on the photocathode of the multiplier tube and which successfully gave rise to photoelectrons. *Lower trace* of each pair shows macroflash recorded from entire cell through substage condenser. The location of the microfield with respect to cytoplasmic structures was documented by a photograph made several seconds prior to photometric recording, and was subsequently indicated in ink. *A*, microfield over nonfluorescent area of cytoplasm. *B*, two closely adjacent, strongly fluorescent organelles within recording field. This specimen was especially well suited for the experiment because of its uncluttered structure.

depicted in Figs. 13 and 14 did indicate a close similarity between the wave shapes of microflashes emitted from different sources. Minor variations in time course were noted among emissions from different sources, but no qualitative differences were found. The organelles flashed with very reproducible intensity-time curves which resembled the macroflash in wave shape, but exhibited slightly shorter rise and decay times.

No latency differences were noted among neighboring microsources. The time which elapses between invasion of a limited region of cytoplasm by the triggering potential and the first signs of light emission from that same area was found to be 2 to 3 msec (Eckert, 1965 *b*). This presumably approximates

the latency between the arrival of the action potential at a microsource and the initiation of the light-producing reaction within the organelle.

Occasionally, even large microsources (as identified by their fluorescence) failed to give a signal above background. When this was the case, none of the organelles within the limited area of the microscope field was found to give signals above background. This regional failure of emission (Fig. 6) was

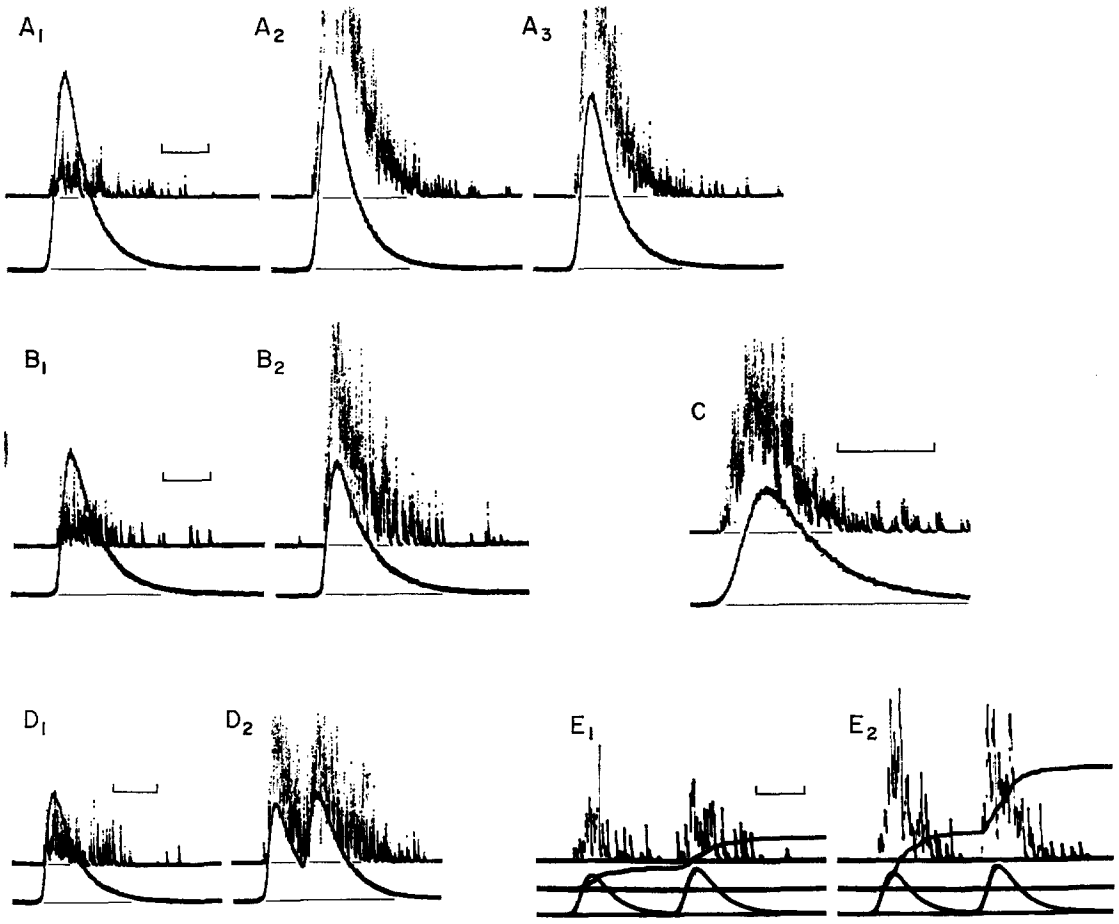

FIGURE 14. Wave shape of the microflash compared with that of the macroflash. Records show signals from medium and large microsources and from adjacent unstructured areas. The microfield signal is displayed on the upper trace, and the macroflash on the lower trace of each frame. A_1, B_1, D_1, and E_1 show background signals, while the remaining frames were recorded with a fluorescent SPRB (microsource) aligned with the microphotometer field. Recording C shows the signal recorded from the pair of organelles in Fig. 13 B at a faster sweep rate for wave shape comparison. Series D and E demonstrate the ability of a microsource to flash in rapid sequence. The middle trace in E is the integrated signal of the upper trace. Each calibration mark is 30 msec.

interpreted as the result of failure of invasion of that region of the cell by the propagated action potential. However, medium and large microsources normally gave an emission well above background. In such cases, the organelles selected for recording consistently responded with each effective (as determined from macroflash display) stimulus. This supports evidence from autophotographic studies (Figs. 9 and 10) that microsources normally respond to each invading action potential.

DISCUSSION

From this study of the light-emitting organelles of *Noctiluca*, termed microsources, a number of deductions and speculations can be made.

It is of interest to note the relationship which exists between the average size of the organelle and the average number of quanta emitted per flash. A diameter of 0.4 μ for the organelle gives a spherical volume of 0.035 μ^3, while an average photon yield for a microflash is 10^5 quanta. If we assume that the enzyme comprises 50% of the organelle, has a molecular weight of 50,000 and a specific density of 1.3 g/cm^3, the number of enzyme molecules calculated for a microsource of average size is 2.7×10^5. Should the molecular weight be greater, or the concentration lower, this value would, of course, have to be correspondingly smaller. Even if each enzyme molecule were associated with the emission of 1 photon per flash, the turnover rate would have to be 10 or more per second to account for the ability to flash in rapid sequence (Fig. 14 *D*, *E*).

The capability of the organelles to flash in rapid sequence implies a control mechanism which limits the luminescence reaction so that following one flash an adequate supply of substrate or precursor remains for additional flashes. There appear to be two major possibilities for the method of control; one of them, control by way of enzyme activity, is employed by the actomyosin system of muscle (Weber et al., 1964; Sandow et al., 1965); in the other the reaction is limited by substrate availability. These will be considered in more detail elsewhere.

The mechanism for the control of luminescence, regardless of its detailed nature, must be presumed to act at the level of the microsource, and must be the last in a sequence of events which couples the luminescence reaction to bioelectric activity. In this regard it is of interest to note that concomitant with short interval potentiation and summation (Eckert, 1965 *a*, Fig. 3) there is no increase in the size of the action potential recorded from the vacuole. Therefore. even though it is impractical to monitor membrane potentials immediately adjacent to an individual microsource under observation, it is reasonable to assume that these also do not increase in amplitude when flash potentiation occurs. Changes in the intensity of the microflash must therefore depend on steps in the coupling sequence which follows the action potential.

It is interesting to consider the possible relationship between the microsource of *Noctiluca* and the birhombohedral crystal (scintillon) associated with luminescence in extracts of *Gonyaulax* (DeSa et al., 1963; Hastings et al., 1966). The active fraction of *Gonyaulax* emits about 10^3 photons per crystal present as compared to about 10^5 per flash from a *Noctiluca* microsource. The difference could be due to loss of substrate or loss of enzyme activity during the isolation of scintillons, or the organelles may be inherently different. The scintillons and microsources are of similar size. Because of its limited resolution, the light microscope cannot reveal the shape of *Noctiluca* microsources; until they have been identified with the electron microscope, structural comparisons of *Noctiluca* microsources with *Gonyaulax* scintillons cannot be made. It should be noted, however, that modest attempts to find birhombohedral crystalline structures in electron micrographs of *Noctiluca* have been unsuccessful. Moreover, the absence of strong birefringence in *Noctiluca* contrasts with the dramatic birefringence of scintillon crystals in *Gonyaulax* (Hastings et al., 1966, Fig. 16).

It is now clear in *Noctiluca* that the intensity-time curve of emission from the whole cell results from nearly synchronous summation of 10^4 or more microflashes, since the time course and shape of the individual microflashes resemble those of the macroflash with only minor differences in duration. The major alternative, that the macroflash results from a characteristic time distribution of brief microsource scintillations, has been ruled out.

The small differences in the measured time course that occur between the micro- and macroflash are not surprising, since microflashes which originate near the region of stimulation are not initiated synchronously with those which arise at more distal portions of the cell. This results from the propagation of the flash-triggering action potential, which conducts over the perivacuolar cytoplasm at about 60 μ per msec (Eckert, 1965 *b*). Microflashes from diverse parts of the cell are normally, therefore, somewhat out of phase with each other, even though their time courses show extensive overlap. Time course differences between micro- and macroflashes are consistent with the 5–10 msec conduction latency for flash initiation at opposite ends of the cell. A shortening of the time course of the macroflash, consistent with this interpretation, occurs when the cell is stimulated in a manner which effects a synchronous triggering of microflashes.[1] The kinetics of the synchronously initiated macroflash shall be considered to represent the average kinetics of all the contributing microsources, with the influence of each microflash weighted in proportion to its intensity.

Evidence from sequences of intensified micrographs (Figs. 9 and 10) indicates that the individual microsource flashes in response to each invading action potential. Measurements of microsource images in serial exposures (Fig. 10) show that there are strong correlations from flash to flash in the

light emitted from different individual microsources. Moreover, these parallel changes in the strength of microsource emissions, which occur in response to irregular stimulus intervals, are similar in degree to changes in the intensities of successive macroflashes which also occur in response to irregular stimulus rate (Nicol, 1958; footnote 1). The reversible changes in the amplitude of the macroflash are therefore the result of graded changes in the amplitudes of microflashes. On the other hand, this evidence argues against recruitment or inactivation of microsources as the physiological basis for macroflash amplitude changes. The exception occurs when progressively larger portions of the cell cease completely to luminesce, presumably due to local failure of invasion by the action potential (Fig. 6). This is an irreversible pathological event, however, and is distinct from physiological differences in flash intensities which are dependent on recovery time between responses.

The success of this work was enhanced by the unfailing care of *Noctiluca* cultures by Miss Francine Brady, and by the very helpful technical assistance of Mr. R. Chaffee. Mr. P. C. Specht helped significantly in the design and construction of the microphotometer. Dr. William Hagins suggested the experiment which resulted in Fig. 11.

Support came from National Science Foundation grant GB-1908, United States Public Health Service grants NB-03664 and NB-05301, and Atomic Energy Commission Contract AT(30-1)-3406.

Received for publication 21 July 1966.

REFERENCES

DESA, R., J. W. HASTINGS, and A. E. VATTER. 1963. Luminescent "crystalline" particles: An organized subcellular bioluminescent system. *Science.* **141**:1269.

ECKERT, R. 1965 *a*. Bioelectric control of bioluminescence in the dinoflagellate *Noctiluca*. I. Specific nature of triggering events. *Science.* **147**:1140.

ECKERT, R. 1965 *b*. Bioelectric control of bioluminescence in the dinoflagellate *Noctiluca*. II. Asynchronous flash initiation by a propagated triggering potential. *Science.* **147**:1142.

ECKERT, R. 1966 *a*. Subcellular sources of luminescence in *Noctiluca*. *Science.* **151**:349.

ECKERT, R. 1966 *b*. Evidence for substrate control of the luminescent flash of *Noctiluca*. *Federation Proc.* **25**:702.

ECKERT, R. 1966 *c*. Excitation and luminescence in *Noctiluca miliaris*. *In* Bioluminescence in Progress. F. A. JOHNSON and Y. HANEDA, editors. Princeton University Press, Princeton. 269.

ECKERT, R., and M. FINDLAY. 1962. Two physiological varieties of *Noctiluca miliaris*. *Biol. Bull.* **123**:494.

ECKERT, R., G. T. REYNOLDS, and R. CHAFFEE. 1965. Microsources of luminescence in *Noctiluca*. *Biol. Bull.* **129**:394.

GROSS, F. 1934. Zur Biologie und Entwicklungsgeschichte von *Noctiluca miliaris*. *Arch. Protistenk.* **83**:178.

HARVEY, E. B. 1917. A physiological study of specific gravity and of luminescence in *Noctiluca*, with special reference to anesthesia. *Carnegie Inst. Wash. Publ.* **251**:253.

HASTINGS, J. W. 1959. Bioluminescence in marine dinoflagellates. *Proc. Nat. Biophys. Conf., 1st. Columbus, Ohio.* 427.

HASTINGS, J. W., M. VERGIN, and R. DESA. 1966. Scintillons: The biochemistry of dinoflagellate bioluminescence. *In* Bioluminescence in Progress. F. A. JOHNSON, and Y. HANEDA, editors. Princeton University Press, Princeton. 301.

KOFOID, C. A., and O. SWEZY. 1921. The Free-Living Unarmored Dinoflagellata. University of California Press, Berkeley.

NICOL, J. A. C. 1958. Observations on luminescence in *Noctiluca. J. Marine Biol. Assoc. U. K.* **37**:535.

PRATJE, A. 1921. *Noctiluca miliaris* Suriray. Beitrage zur Morphologie, Physiologie and Cytologie. I. Morphologie und Physiologie. *Arch. Protistenk.* **42**:1.

QUATREFAGES, A. DE. 1850. Observations sur les noctiluques. *Ann. Sci. Nat. Zool. Ser. 3.* **14**:236.

REYNOLDS, G. T. 1964. Evaluation of an image intensifier system for microscopic observations. *IEEE (Inst. Elec. Electron. Eng.) Trans. Nucl. Sci.* **11**:147.

REYNOLDS, G. T. 1966 *a.* Sensitivity of an image intensifier film system. *J. Appl. Optics.* **5**:577.

REYNOLDS, G. T. 1966 *b.* Secondary electron multiplication in image intensifier dynode structures. *IEEE (Inst. Elec. Electron. Eng.) Trans. Nucl. Sci.* **13**:81.

REYNOLDS, G. T., and P. BOTOS. 1965. Sensitivity of image intensifier-film systems for observing weak light sources. Technical Report No. 1. Princeton University Contract AT (30-1)-3406.

SANDOW, A., S. R. TAYLOR, and H. PREISER. 1965. Role of the action potential in excitation-contraction coupling. *Federation Proc.* **24**:1116.

SHEINGOLD, D. H. 1964. Impedance and admittance transformations using operational amplifiers. *Lightening Empiricist.* **12**:1.

STREHLER, B. L., and W. D. MCELROY. 1949. Purification of firefly luciferin. *J. Cellular Comp. Physiol.* **34**:457.

SWEENEY, B. M., and G. B. BOUCK. 1966. Crystal-like particles in luminous and nonluminous dinoflagellates. *In* Bioluminescence in Progress. F. A. JOHNSON and Y. HANEDA, editors. Princeton University Press, Princeton. 331.

WEBER, A., R. HERZ, and I. REISS. 1964. The regulation of myofibrillar activity by calcium. *Proc. Roy. Soc. (London), Ser. B.* **160**:489.